Journal of
Synchrotron Radiation

ISSN 0909-0495

Received 10 December 2005
Accepted 24 February 2006

X-ray diffractometer combining synchrotron radiation and pulsed magnetic fields up to 40 T

Y. Narumi,[a]* K. Kindo,[a] K. Katsumata,[b] M. Kawauchi,[c] Ch. Broennimann,[d] U. Staub,[d] H. Toyokawa,[e] Y. Tanaka,[b] A. Kikkawa,[b] T. Yamamoto,[c] M. Hagiwara,[c] T. Ishikawa[b] and H. Kitamura[b]

[a]ISSP, University of Tokyo, Kashiwa, Chiba 277-858, Japan, [b]RIKEN SPring-8 Center, Harima Institute, Sayo, Hyogo 679-5148, Japan, [c]KYOKUGEN, Osaka University, Toyonaka, Osaka 560-8531, Japan, [d]Swiss Light Source, Paul Scherrer Institut, 5232 Villigen, Switzerland, and [e]SPring-8/JASRI, Sayo, Hyogo 679-5198, Japan. E-mail: narumi@issp.u-tokyo.ac.jp

A synchrotron X-ray diffractometer incorporating a pulsed field magnet for high fields up to 40 T has been developed and a detailed description of this instrument is reported. The pulsed field magnet is composed of two coaxial coils with a gap of 3 mm at the mid-plane for passage of the X-rays. The pixel detector PILATUS 100K is used to store the diffracted X-rays. As a test of this instrument, X-ray diffraction by a powder sample of the antiferromagnet CoO is measured below the Néel temperature. A field-dependent lattice distortion of CoO due to magnetostriction is observed up to 38 T.

Keywords: X-ray diffraction; pulsed high magnetic field; pixel detector; magnetostriction; antiferromagnet.

1. Introduction

The study of materials by X-ray diffraction techniques using third-generation synchrotron sources has been performed extensively in recent years. Studies of magnetic materials are an example of a discipline that has particularly benefited from techniques making use of synchrotron radiation. In studying the properties of magnetic materials, it is useful to change the temperature, T, and/or applied magnetic field, B, in the measurements. Various new phenomena may appear at high fields (for a review, see Berthier *et al.*, 2002) which can be studied by X-ray diffraction techniques. We have developed a high-field and low-temperature facility in conjunction with an X-ray diffractometer at the synchrotron source SPring-8 at Harima, Japan (Katsumata, 2005). At this facility a split-pair superconducting magnet up to 15 T is used in conjunction with a dilution refrigerator. In order to obtain a magnetic field of 15 T at the sample position by this split-pair magnet, each coil should generate a higher magnetic field of $\sim$20 T, which is close to the limit of modern superconductor technology. The magnetic field could be increased by a few more teslas using new materials such as high-temperature superconductors. In order to achieve much higher fields, a hybrid magnet or a pulsed field magnet is needed (for a review, see Herlach & Miura, 2003). A hybrid magnet, in which a water-cooled resistive magnet is inserted into a superconducting magnet, requires a large space for the installation as well as a facility for cooling. Therefore, a hybrid magnet is not suitable for synchrotron X-ray experiments. On the other hand, a pulsed field magnet can be placed on the goniometer with a relatively small power source. Moreover, the synchrotron X-ray beam is bright enough for time-resolved data collecting, which is inevitable in experiments exploiting pulsed magnetic fields. A synchrotron X-ray diffraction measurement under pulsed fields up to 20 T has been reported and the field dependence of the lattice distortion in $Pr_{1-x}Ca_xMnO_3$ ($x \simeq 0.4$) has been measured up to 16 T (Matsuda *et al.*, 2004). In this paper we report technical details of our new X-ray diffractometer with pulsed high magnetic fields up to 40 T.

2. Apparatus

2.1. General considerations

Our diffractometer is installed at the beamline BL19LXU (Yabashi *et al.*, 2001) at SPring-8. This beamline is equipped with a 27 m-long undulator (Hara *et al.*, 2002) providing a flux of X-rays that is five times stronger than at any other beamline with a 5 m undulator at SPring-8. The X-ray beam of BL19LXU yields sufficient flux and energy resolution in the ranges 7–19 keV, 23–56 keV and 38–94 keV, utilizing the first, third and fifth harmonics, respectively, for typical experiments. A Si(111) double-crystal monochromator equipped with a cryogenic cooling system for high heat load is located in the optics hutch. Four experimental hutches are arranged in a tandem fashion and our hutch (#4) is located at the end of the beamline at approximately 135 m from the center of the undulator. The incident beam size in the experimental hutch is 1 mm $\times$ 2 mm and the estimated photon flux is $\sim 5 \times 10^{13}$ photons s^{-1} for an X-ray energy of 30 keV. For a typical

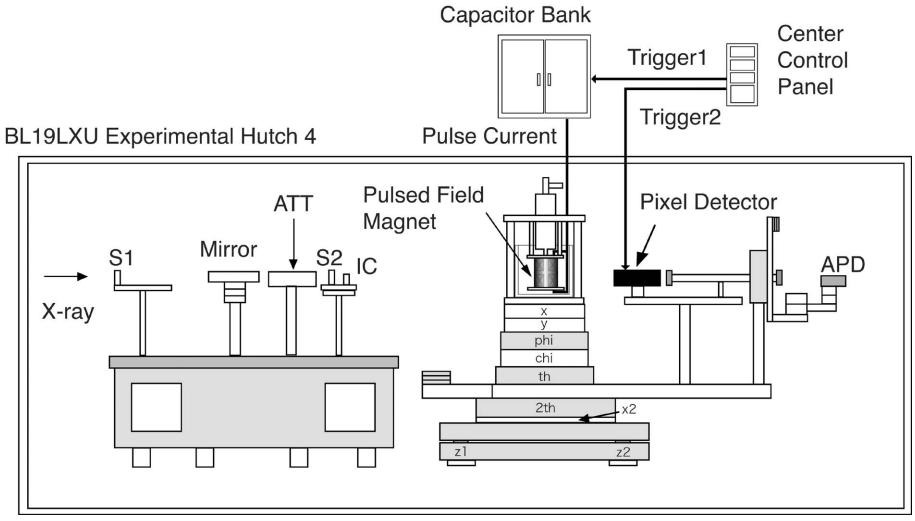

Figure 1
Schematic view of the X-ray diffractometer installed in experimental hutch #4 of the beamline BL19LXU at SPring-8 with a pulsed field magnet and power supply. A cryostat can be inserted into the magnet.

Bragg reflection from a single crystal the intensity of the diffracted beam is $\sim 10^9$ photons s^{-1} and $\sim 10^3$ photons μs^{-1}. Consequently, an X-ray diffraction measurement using a pulsed field with a pulse duration of a few milliseconds becomes feasible at this beamline.

2.2. Diffractometer

Fig. 1 shows schematically the diffractometer installed at experimental hutch #4. Incident X-rays come from the left-hand side of the figure and are reflected by a Pt-coated Si mirror with an angle of 0.1° to eliminate higher harmonic X-rays. An attenuator (ATT), composed of Cu and Al plates of various thicknesses, can be inserted in front of the sample. The reflected X-rays are introduced to the four-circle goniometer manufactured by Huber, Germany, with the 2θ (2th), θ (th), χ (chi) and φ (phi) rotations, in which the χ rotation is limited to $\pm 5°$. Here we define the z axis upwards, the x axis perpendicular to the plane of the paper in Fig. 1, and the y axis along the direction of the beam. The vertical and horizontal positions of the entire goniometer are adjusted by the $z1$ and $z2$ motors and the $x2$ motor in Fig. 1, respectively. The 2θ arm (2th) rotates in the horizontal plane (the xy plane). The position of the sample table, which is on the φ circle (phi), is adjusted by two translations, x and y. All components of the goniometer, including the worm gears and ball bearings, are made of non-magnetic materials. In addition, all the motors are more than 70 cm away from the center of the magnet, and their function is not affected by stray fields.

X-rays diffracted by the sample are detected by either a pixel detector or an avalanche photodiode (APD). In this study we used a novel single-photon-counting pixel detector called PILATUS 100K that was developed at the Swiss Light Source (Hülsen *et al.*, 2005). The PILATUS 100K single-module detector consists of an array of 487 × 197 pixels, with a pixel size of 0.172 mm × 0.172 mm. Each pixel is operated in single-photon-counting mode, *i.e.* only X-rays above a certain threshold energy are counted. Pixels feature 20-bit counters, *i.e.* up to 10^6 photons can be counted in a pixel per exposure. The outstanding features of the detector are: (i) no noise contribution owing to dark current or read-out noise leading to an excellent signal-to-noise ratio, (ii) short readout time of ~5 ms, (iii) electronic gating, *i.e.* synchronization of the shutter signal with an external trigger is easily performed, and (iv) very simple operation at room temperature. The detector was operated with its threshold energy set to 12 keV which is significantly below the X-ray energy of 24 keV used in the measurements. The detector was mounted on the 2θ arm of the diffractometer at a distance of 50 cm from the sample. In this geometry the angular resolution corresponding to the pixel size is approximately 0.018° in 2θ.

2.3. Pulsed field magnet

The pulsed field magnet used in this study is a split-pair based on the non-destructive solenoid coil design developed by Kindo and collaborators (Kindo, 2001). Fig. 2 shows a schematic cross section of the magnet.

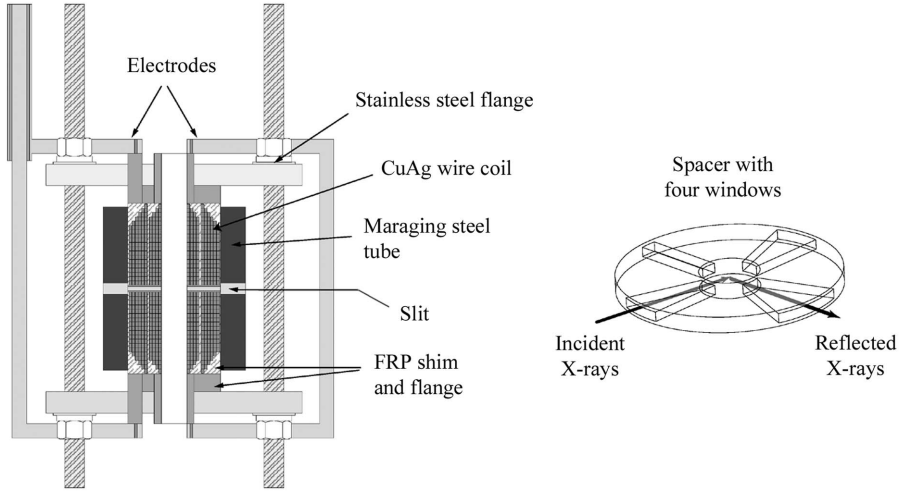

Figure 2
Cross section of the pulsed field magnet for the X-ray diffraction measurement (left) and a schematic view of the spacer inserted between the two coils (right).

We have made three magnets (#1, #2 and #3) with similar size (the coils have ~65 mm diameter and ~150 mm axial length). The #1 magnet has a spacer between the two coils made of a fiber-reinforced plastic, the #2 magnet has a stainless steel spacer, and the #3 magnet has a spacer made of Maraging steel. The magnet has an 18 mm cold bore and four windows with a slit width of 3 mm for passage of the X-ray beam. Each coil consists of ten layers of coaxially wound CuAg wires with a 2 mm × 3 mm cross section coated with a Kapton sheet for insulation. This wire, manufactured by Showa Electric Wire & Cable, contains 24 wt.% Ag and has a tensile strength of 900 MPa. The two coils, with a spacer between them, are inserted into a Maraging steel tube for reinforcement. This tube is equipped with four windows that align with the windows in the spacer, and it has an inner diameter of 67 mm, outer diameter of 100 mm and height of 150 mm. Maraging steel has a tensile strength of 2200 MPa. The magnet is immersed in a liquid-nitrogen bath to decrease the resistance and to remove heat generated by the electric discharge. With a capacitor bank of 5 mF and 160 kJ, magnetic fields up to 42 T are obtained in the #2 magnet with a pulse duration of 5.5 ms, as shown in Fig. 3. Fig. 4 shows the measured distribution of the magnetic field along the vertical axis of the #2 magnet. The homogeneity is about 5% within ±5 mm from the center of the coil. A cryostat made of glass can be inserted into the magnet and the sample temperature can be lowered to liquid-helium temperatures.

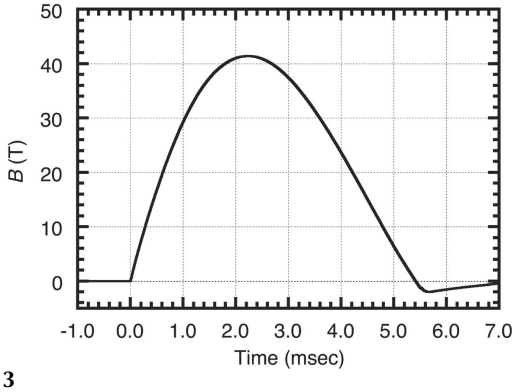

Figure 3
Time variation of the pulsed magnetic field measured in the #2 magnet.

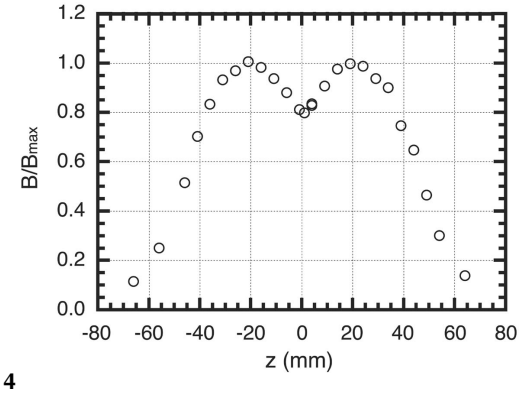

Figure 4
Change in the magnetic field with distance from the center of the coil along the vertical axis of the #2 magnet.

3. Example of a measurement

In order to test the performance of the apparatus, we have carried out Bragg diffraction measurements on CoO, a typical example of an antiferromagnet with cubic structure above the magnetic ordering temperature, T_N = 290 K. The ground state of a free Co^{2+} ion is ^4F. In a cubic crystal field Co^{2+} has a triply degenerate orbital ground state. The orbital angular momentum is not fully quenched, and these properties of CoO are sensitive to lattice distortion. Below T_N the crystal structure changes from cubic to tetragonal (Tombs & Rooksby, 1950), with space group *I*4/*mmm* and lattice constants a = 3.015 Å and b = 4.2143 Å (Villars & Calvert, 1985). This phenomenon, known as magnetostriction, occurs to gain the magnetic energy at the cost of lattice energy (for a review see Kanamori, 1963). Nakamichi observed the field-dependent magnetostriction on a single crystal of CoO up to 1.1 T using a strain gauge (Nakamichi, 1965).

We measured X-ray diffraction by a powder sample of CoO under pulsed high magnetic fields. The powder sample was purchased from Sigma-Aldrich and had a purity of 99.99%. Fig. 5 shows the timing chart for the measurement. Before the pulsed field is applied, an X-ray diffraction pattern is recorded in zero field for 10 ms. After waiting for 1 s, a trigger pulse is applied to discharge the capacitor bank through the magnet. An X-ray diffraction image is stored for 1 ms after waiting for 1.7 ms from the trigger. The second exposure is carried out at a time interval where the variation of the magnetic field is at a minimum. During this exposure the magnetic field changes by about 5%. A final exposure of 10 ms after another delay of 1 s is used to confirm the zero field data. The change in the field of ~5% owing to the chosen time window of 1 ms leads to a scatter in the distribution of crystal lattice planes. This distribution increases the line width of the reflections by a few %, which is below the limit of our detection. Therefore, the exposure time can be chosen such that the collected statistics are optimized compared with the width of the reflection. Fig. 6 shows an image of the powder diffraction rings taken at a magnetic field B = 20 T and a temperature T = 160 K.

To analyze the shift of the diffraction peaks as a function of applied magnetic field, all three data sets from the exposures shown in Fig. 5 were fitted with a Voigt function. The Bragg position under an applied field, including the zero-field calibration pattern, was then subtracted from the average of the

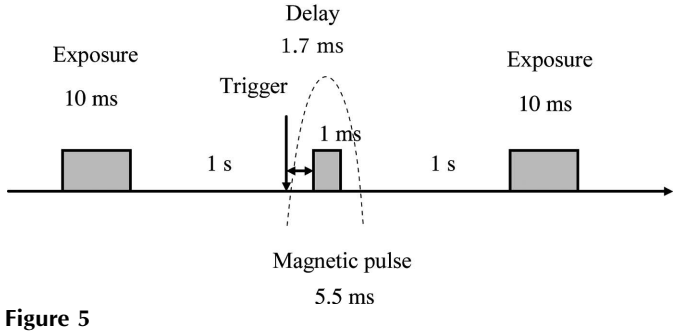

Figure 5
Timing chart for the X-ray diffraction measurement under a pulsed magnetic field.

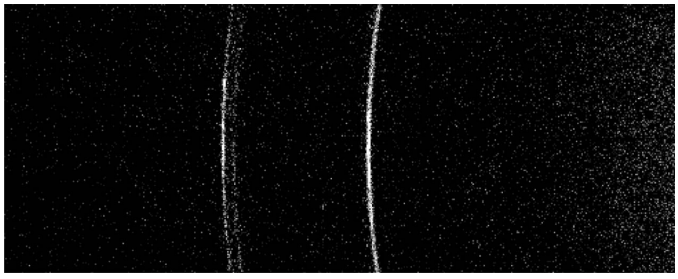

Figure 6
Image of the powder diffraction pattern of CoO obtained at $B = 20$ T and $T = 160$ K. These rings come from the (002) ($2\theta = 17.81^\circ$), (110) ($2\theta = 17.65^\circ$) and (101) ($2\theta = 15.83^\circ$) reflections, respectively, from the left to the right. The energy of the incident X-rays is 24 keV.

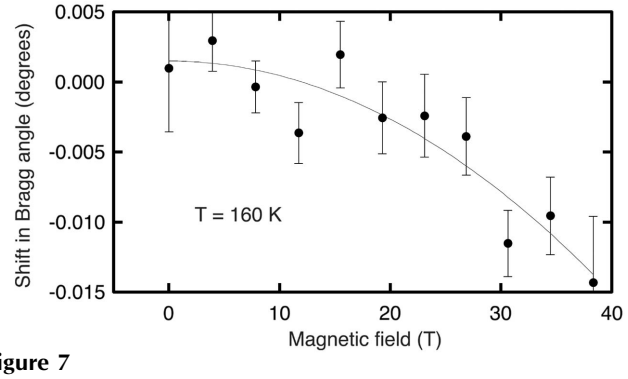

Figure 7
Magnetic field dependence of the (110) Bragg position of CoO measured at $T = 160$ K. The vertical axis shows the difference in 2θ between zero and the finite fields. The full curve shows a fit to the data with 1.5×10^{-3}–1.0×10^{-5} B^2.

two zero-field data sets. Fig. 7 shows the change in the (110) Bragg position with magnetic field measured at $T = 160$ K. We were able to follow the change of the Bragg reflection up to 38 T. To the best of our knowledge, this is the highest magnetic field achieved to date in an X-ray diffraction measurement. A full description and analysis of the results will be reported elsewhere.

4. Conclusions and future direction

We have developed an X-ray diffractometer equipped with a very high magnetic field facility. This diffractometer will be useful for the study of magnetic materials and superconductors, since many novel phenomena are expected to occur at high fields (for a review, see Berthier *et al.*, 2002 and Herlach & Miura, 2003). A magnet consisting of a single solenoid coil is easier to construct than the split-pair magnet. However, the Bragg angle for such a single-coil magnet is limited and it is not suitable for diffraction measurements. Although the split-pair magnet is not easy to design, it has a great advantage over the solenoid magnet in that a scan over a wide range of reciprocal lattice space can be performed. In the case of a split-pair magnet, a strong attractive force is exerted between the two coils which limits the magnetic field available with it. We tested the #2 magnet and it was degraded at about 48 T. At the same time the spacer made of stainless steel was severely compressed. In order to avoid this damage, we employed a spacer made of Maraging steel and have been successful as described above.

We are planning to increase the energy of the capacitor bank which will increase both the peak field and the pulse duration of the field. Doubling the energy and a new design of a coil will increase the peak field to $\sim$50 T and the pulse duration to $\sim$10 ms. A longer pulse duration makes the measurement easier of course. It is possible to insert a dilution fridge into the magnet as demonstrated by Kindo (2001) in the case of a solenoid coil. Heating of the sample by pulsed fields is not a serious problem in insulating samples. In metallic samples, depending on the conductivity, we use a powder sample or a pillar-shaped single crystal to reduce the heating. In the near future it may become possible to conduct an X-ray diffraction measurement up to $\sim$60 T at a temperature as low as $\sim$50 mK.

When a pixel detector with higher readout time becomes available, time-resolved measurements will be feasible. For example, if we take a two-dimensional image within a few microseconds, then a diffraction pattern could be stored during the field pulse with a resolution of $\sim$0.04 T. Using this technique it will be possible to study the time dependence of a magnetic phase transition in applied magnetic fields and many other time-dependent phenomena.

We would like to thank S. W. Lovesey for useful comments. This work was partially supported by a Grant-in-Aid for Scientific Research from the Japan Society for the Promotion of Science.

References

Berthier, C., Lévy, L. P. & Martinez, G. (2002). Editors. *High Magnetic Fields, Applications in Condensed Matter Physics and Spectroscopy*. Berlin: Springer.
Hara, T., Yabashi, M., Tanaka, T., Bizen, T., Goto, S., Maréchal, X. M., Seike, T., Tamasaku, K., Ishikawa, T. & Kitamura, H. (2002). *Rev. Sci. Instrum.* **73**, 1125–1128.
Herlach, F. & Miura, N. (2003). *High Magnetic Fields, Science and Technology*. Singapore: World Scientific.
Hülsen, G., Brönnimann, Ch. & Eikenberry, E. F. (2005). *Nucl. Instrum. Methods*, A**548**, 540–554.
Kanamori, J. (1963). *Magnetism*, Vol. 1, edited by G. T. Rado and H. Suhl, pp. 189–199. New York: Academic Press.
Katsumata, K. (2005). *Phys. Scr.* **71**, CC7–13.
Kindo, K. (2001). *Physica B*, **294–295**, 585–590.
Matsuda, Y. H., Ueda, Y., Nojiri, H., Takahashi, T., Inami, T., Ohwada, K., Murakami, Y. & Arima, T. (2004). *Physica B*, **346–347**, 519–523.
Nakamichi, T. (1965). *J. Phys. Soc. Jpn*, **20**, 720–726.
Tombs, N. C. & Rooksby, H. P. (1950). *Nature (London)*, **165**, 442–443.
Villars, P. & Calvert, L. D. (1985). *Pearson's Handbook of Crystallographic Data for Intermetallic Phases*, Vol. 1, pp. 473. Ohio: American Society for Metals.
Yabashi, M., Mochizuki, T., Yamazaki, H., Goto, S., Ohashi, H., Takeshita, K., Ohata, T., Matsushita, T., Tamasaku, K., Tanaka, Y. & Ishikawa, T. (2001). *Nucl. Instrum. Methods*, A**467–468**, 678–681.